ORAL SURGERY
ORAL MEDICINE
ORAL PATHOLOGY

ENDODONTICS *Editor: Larz M.S. Spångberg*

A mouse model of inflammatory root resorption induced by pulpal infection

Khaled Balto, BDS,[a] Robert White, DMD,[b] Ralph Mueller, PhD,[c] and Philip Stashenko, DMD, PhD,[d] Boston, Mass
FORSYTH INSTITUTE, UNIVERSITY ZURICH, AND HARVARD UNIVERSITY

Objective. The present study was undertaken to determine the frequency and extent of apical root resorption associated with induced periradicular lesions in mice.
Study design. Bone and root resorption was quantified by using two- and three-dimensional micro–computed tomography (μ-CT) in the lower first molars of mice subjected to pulp exposure and infection.
Results. μ-CT measurements showed significant apical resorption in exposed and infected teeth, resulting in an average distal root shortening of 12.7% ($P < .001$ vs unexposed). These findings were confirmed with three-dimensional reconstituted images that showed thinning and shortening of the distal root. Tartrate-resistant acid phosphatase clastic cells were associated with resorption lacunae on the cementum of root apices, as well as on bone at the periphery of the periradicular lesions. Brown and Brenn staining showed the presence of bacteria in dentinal tubules adjacent to resorbed cementum.
Conclusions. Apical root resorption is a prominent and consistent finding associated with periradicular infection in the mouse. This species represents a convenient model for studying the pathogenesis of inflammatory root resorption in vivo.
(Oral Surg Oral Med Oral Pathol Oral Radiol Endod 2002;93:461-8)

The resorption of bone surrounding the roots of teeth is a pathologic consequence of dental pulp infection.[1,2] Microbial products elicit host inflammatory and immune responses, particularly the expression of proinflammatory cytokines that stimulate the formation and activation of osteoclasts.[2-4] The concomitant resorption of the hard tissues of the tooth, including cementum and dentin, may also occur during this process and can result in the loss of considerable root structure and in reduced tooth stability.[5-7]

Supported by grants DE-09018, DE-11664, DE-13747, and AG-13333 from the National Institutes of Health and the M. E. Muller Professorship in Bioengineering at Harvard Medical School.
[a]Postdoctoral Fellow, Department of Cytokine Biology, Forsyth Institute, and Division of Endodontics, Harvard School of Dental Medicine.
[b]Postdoctoral Program Director, Division of Endodontics, Harvard School of Dental Medicine.
[c]SNF Professor of Bioengineering, Institute for Biomedical Engineering, ETH and University of Zurich.
[d]Senior Staff Member, Department of Cytokine Biology, Forsyth Institute.
Received for publication Oct 26, 2001; returned for revision Nov 7, 2001; accepted for publication Dec 4, 2001.

1079-2104/2002/$35.00 + 0 **7/15/122641**
doi:10.1067/moe.2002.122641

Rodent models have proved useful for studies of the pathogenesis of periradicular bone resorption. After surgical pulp exposure and deliberate infection, bone destruction occurs rapidly, with highly reproducible kinetics during a 7- to 21-day period.[8,9] The mediators implicated in stimulating resorption include interleukin-1α (IL-1α) and IL-1β.[3,4,10] Resorption is significantly inhibited by the endogenous expression of anti-inflammatory mediators such as IL-6 and IL-10.[10,11]

Clinically, the presence of apical root resorption is usually detected by using radiographic techniques. However, radiographic measures of the extent of root resorption usually underestimate the extent of resorption as determined by the histology of affected teeth.[12] Recently, we have shown that a novel imaging technology, micro–computed tomography (μ-CT), is a rapid, reproducible, and noninvasive method for the determination of periradicular lesion size in the mouse model.[13] μ-CT gives results that are closely comparable to those obtained by histology. The potential also exists for three-dimensional reconstruction of tooth structure, which may permit μ-CT to be used to accurately assess the severity of root resorption.

The purpose of the present study was to use μ-CT to determine the frequency and extent of root resorption

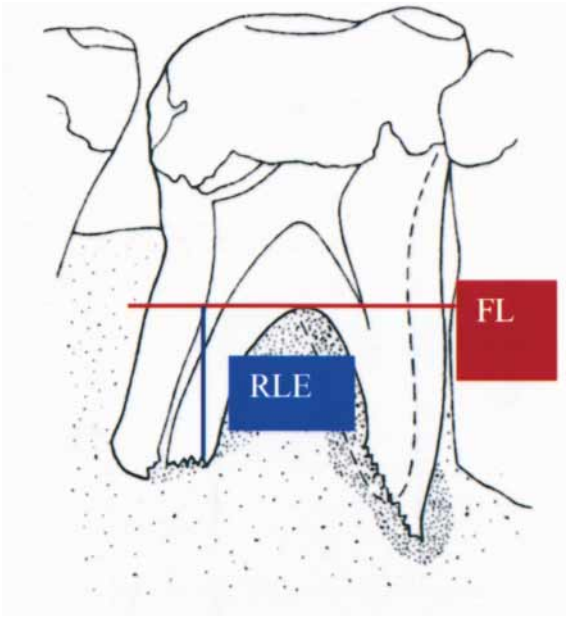

Fig 1. Methodology for determining root length. A perpendicular line (*RLE*) was constructed from the *FL* to the shortest portion of the distal root end.

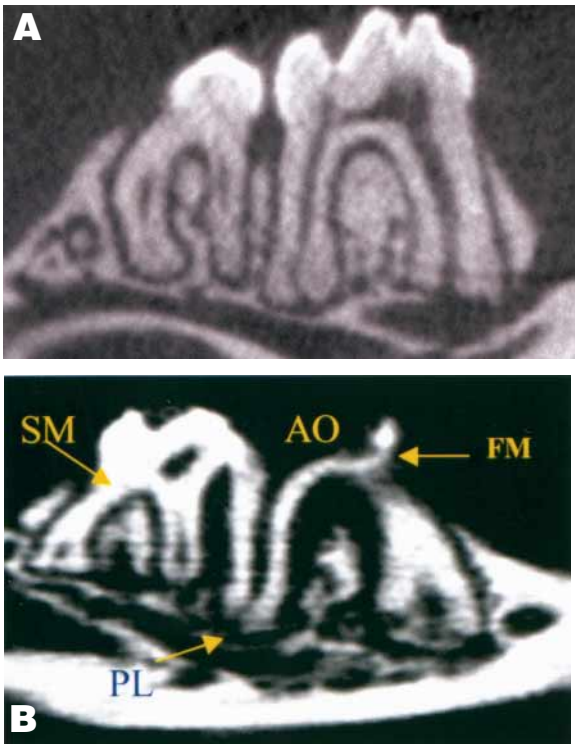

Fig 2. Two-dimensional μ-CT image of the first molar. **A**, Control, noninfected tooth; **B**, experimental, infected tooth. *FM*, First molar; *AO*, access opening; *PL*, periradicular lesion.

associated with induced inflammatory periradicular bone destruction in the mouse model.

MATERIAL AND METHODS

Animals

Eleven-week-old C57BL6 male mice (n = 7) were obtained from Charles River Breeding Laboratory, Wilmington, Mass, and were maintained in a conventional environment in the Forsyth Institute Animal Facility according to the guidelines of the Institutional Animal Care and Use Committee.

Periradicular lesion induction

For lesion induction, mice (n = 5) were mounted on a jaw retraction board and anesthetized with ketamine HCl (62.5 mg/kg) and xylazine (12.5 mg/kg) in sterile phosphate-buffered saline by intraperitoneal injection. All lower first molar pulps were exposed to the oral environment by using a #1/4 round bur under a surgical microscope (model MC-M92; Seiler, St Louis, Mo). The exposure site was approximately equivalent to the diameter of the bur. The pulp chamber was opened until the entrances of the canals could be visualized and probed with an 06 endodontic file. Animals without exposures (n = 2) served as controls.

Infection with pathogens

Trypticase soy broth with yeast agar plates of 4 common endodontic pathogens, *Prevotella intermedia* ATCC 25611, *Streptococcus intermedius* ATCC 27335, *Fusobacterium nucleatum* ATCC 25586, and *Peptostreptococcus micros* ATCC 33270 were grown under anaerobic conditions (80% N_2, 10% H_2, and 10% CO_2), harvested, and cultured in *Mycoplasma* liquid media. The cells were centrifuged at 7000*g* for 15 minutes and resuspended in prereduced anaerobically sterilized Ringer solution. The final concentration of each organism was determined by using a spectrophotometer, and the 4 pathogens were mixed to yield a concentration of 10^{10} cells of each pathogen/mL in 10 μg methyl cellulose/mL. A total of 1 to 2 μL/tooth was introduced by using a micropipette.

Sample preparation

All animals were killed by CO_2 asphyxiation on day 21 after pulp exposure. The mandibles were dissected free of soft tissue, fixed in 10% phosphate-buffered formalin, and subjected to μ-CT. After μ-CT image acquisition, the mandibles were demineralized in 14% ethylenediaminetetraacetic acid, pH 7.2, at room temperature for 3 weeks. Samples were embedded in paraffin, and 7-μm thick sections were prepared. Sections were stained with hematoxylin-eosin, Brown and Brenn, and tartrate-resistant acid phosphatase (TRAP).

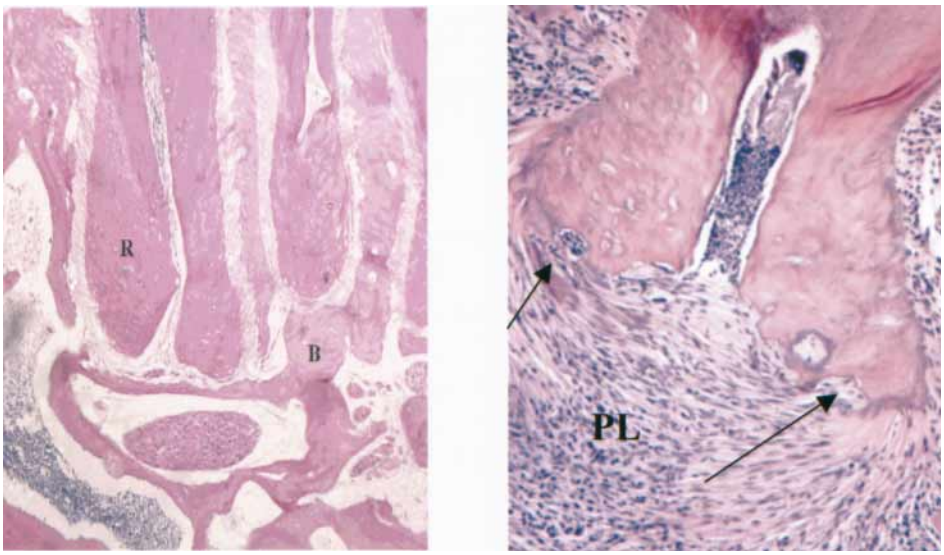

Fig 3. Photomicrograph of representative histologic section of distal root of lower first molar in a mouse. **A**, Control; **B**, exposed, infected tooth. *R*, Root; *B*, bone; *PL*, periradicular lesion. *Black arrows* indicate resorption lacunae.

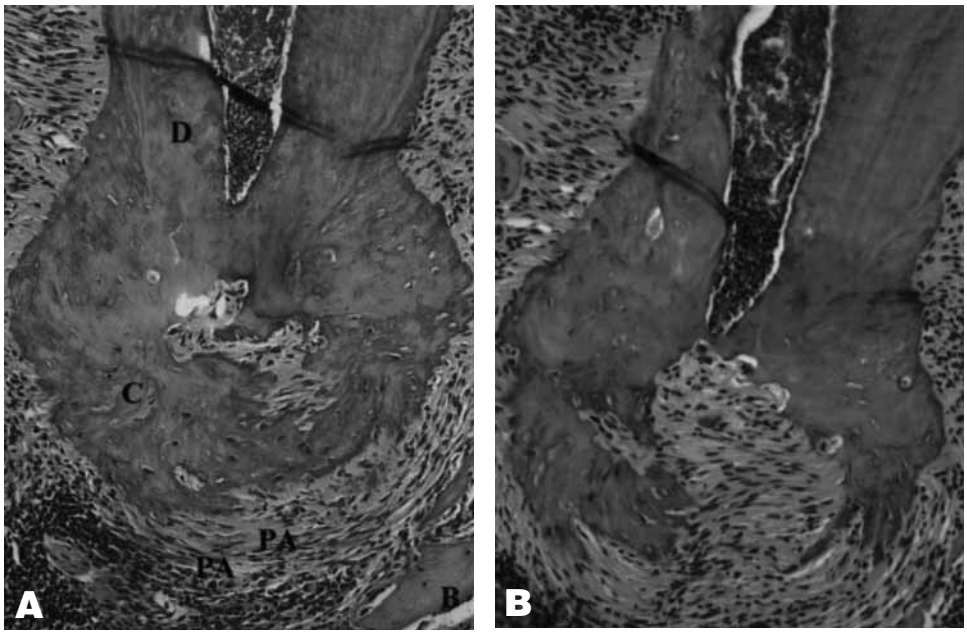

Fig 4. Photomicrograph of representative histologic sections (**A, B**) 30 μm apart illustrating resorption of apical cementum. *D*, Dentin; *C*, cementum; *PA*, periapical lesion; *B*, bone.

Micro–computed tomography

μ-CT was used to quantify the extent of both bone and root resorption. Fixed mandibular samples were analyzed by using a compact fan-beam–type tomograph (μCT 20; Scanco Medical AG, Bassersdorf, Switzerland). For each sample approximately 150 micro-tomographic slices with an increment of 17 μm were acquired, covering the entire mediolateral width of the mandible. From the three-dimensional stack of μ-CT images, a "pivot" section was selected that included the crown and central portion of the distal root of the mandibular first molar.[3] The cross-sectional area of the region of interest was analyzed with a semiautomatic histomorphometric system (Optimas Bioscan; Media Cybernetics, Bethell, Wash).

Quantification of periradicular lesions

The area of evaluation included the area of periradicular destruction (mm^2) and/or the periodontal ligament

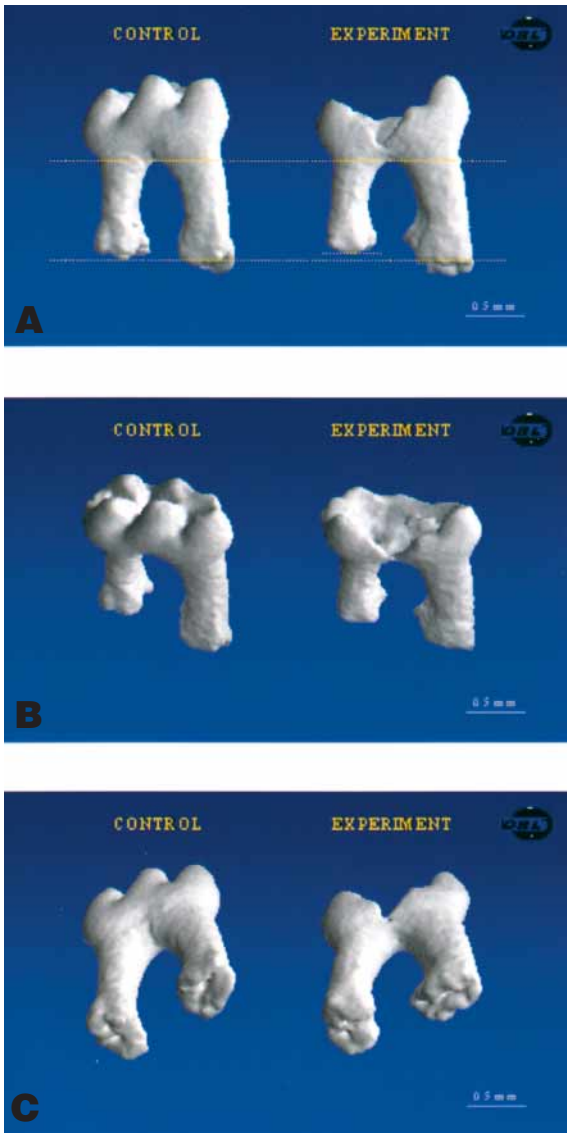

Fig 5. Reconstituted μ-CT images of the mouse first molar. Note the difference in architecture between the apex of the distal root of a control *(left, arrow)* and an experimental root *(right)*. **A**, Sagittal view; **B**, superior view; **C**, inferior view.

space surrounding the distal root of the first molar, the coronal extension of which was standardized by means of a predrawn template.[13]

Determination of root resorption

For measuring the amount of root resorption, 2 landmarks were identified on the μ-CT images of each tooth, the superior border of the furcation area and the shortest length of the tooth apex (Fig 1). The furcal line (FL) was extended to the mesial and distal margins of the tooth. The root length was measured as the distance from the FL to the closest point on the root apex in the experimental (RE) or the control (RC). Each section was measured twice by 2 evaluators who were blinded to the sections being examined.

Table I. Root length in control and experimental teeth

Group	*Root length (mm^2)*
Control	1.380 ± 0.049
Experimental	1.247 ± 0.142*

Data are expressed as mean ± standard deviation.
*P = .014.

For the three-dimensional reconstruction of the distal root, after sample preparation for μ-CT image acquisition, the mandibular samples were measured by μ-CT at 60 kV. Typically 150 to 300 slices with a voxel size of 17 × 17 × 17 μm were scanned, with each scanning procedure requiring 4 to 6.5 hours. Each slice was 17-μm thick in superior-inferior direction (coronal-apical direction).

The volume of interest extended from the superior margin of the root down to its inferior border at the root end. The original gray scale images were then processed with a slight gaussian low-pass filtration for noise reduction and a fixed threshold to separate roots from the surrounding bony structures. These procedures produced binary images of the tooth. The high contrast of dentin to thymol-filled root canals with a linear attenuation ratio of roughly 8 yielded excellent segmentation of the specimens. After image acquisition, the geometric shape of the root ends was characterized from superior, inferior, and lateral directions.

Statistical analysis

The descriptive statistics, including the mean and standard deviation for periradicular lesion size, as well as the amount of root resorption were calculated. Differences in bone destruction and root length in the experimental and control groups were analyzed by *t* test. The correlation between periradicular lesion size and root resorption was tested by regression analysis.

RESULTS

Periradicular lesions in infected and noninfected control teeth

Pulp exposure and infection with a mixture of 4 endodontic pathogens were carried out in the experimental group of mice, whereas control mice remained unexposed and uninfected. After 21 days, control teeth without pulp exposures had a narrow periodontal ligament space and normal periradicular bony architecture (Fig 2, *A*). In contrast, teeth with exposures and infection exhibited readily discernible radiolucencies surrounding the mesial and distal root apices (Fig 2, *B*). The extent of bony destruction was determined from two-dimensional μ-CT images of the lesion area. As expected, teeth with

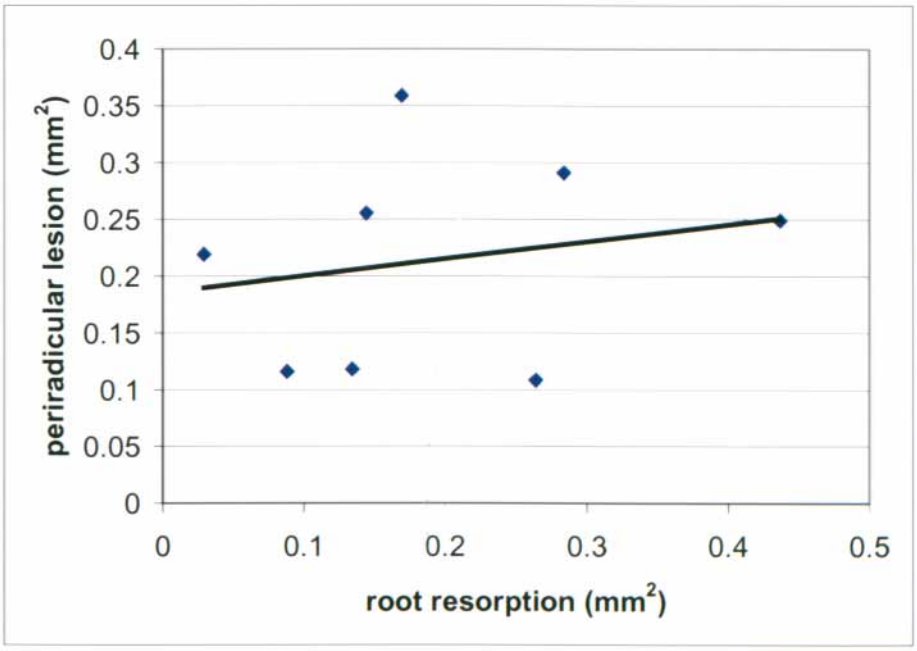

Fig 6. Correlation between periradicular bone resorption and apical root resorption as determined by regression analysis. R^2 value *(top left corner)* indicates a significant relationship.

pulp exposures had significantly more periradicular bone destruction compared with controls ($P < .0001$) (data not shown).

Root resorption in experimental and control teeth

As seen in the μ-CT images, the root of the lower incisor extends from the posterior region of the mandible to the anterior incisal area and is located just inferior to the molar root apices, leaving a limited area for the expansion of the bony lesion. Because periradicular lesions are not seen to expand into the incisive canal, this suggests that lesion expansion may occur at the expense of the root structures as well as the surrounding bone.

Examination of histologic sections suggested the presence of destructive changes involving the root apices of infected teeth. As shown in Fig 3, *B*, roots in the experimental group showed irregular architecture and the presence of numerous resorption lacunae. In some sections the resorption of cementum and dentin was extensive (Fig 4). In contrast, the distal roots of the control group were blunt ended with uniform architecture (Fig 3, *A*). These observations were further confirmed by comparing the reconstructed three-dimensional images of the lower first molar by using μ-CT. In the sagittal sections (Fig 5, *A*), the experimental teeth showed a thinning and significant length reduction of the distal root of the first molar. This was better shown in the inferior-superior and the superior-inferior projections (Fig 5, *B* and *C*) in which the distal processes, clearly visible in the control specimens, were resorbed in the experimental group with a more rounded appearance of the root.

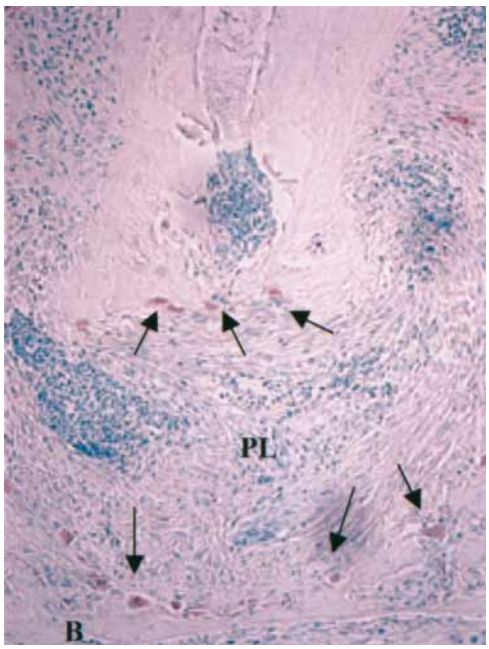

Fig 7. Photomicrograph of histologic section stained with TRAP. *Arrows* indicate $TRAP^+$ cells (red) on the root end and on bone at the periphery of the periradicular lesion.

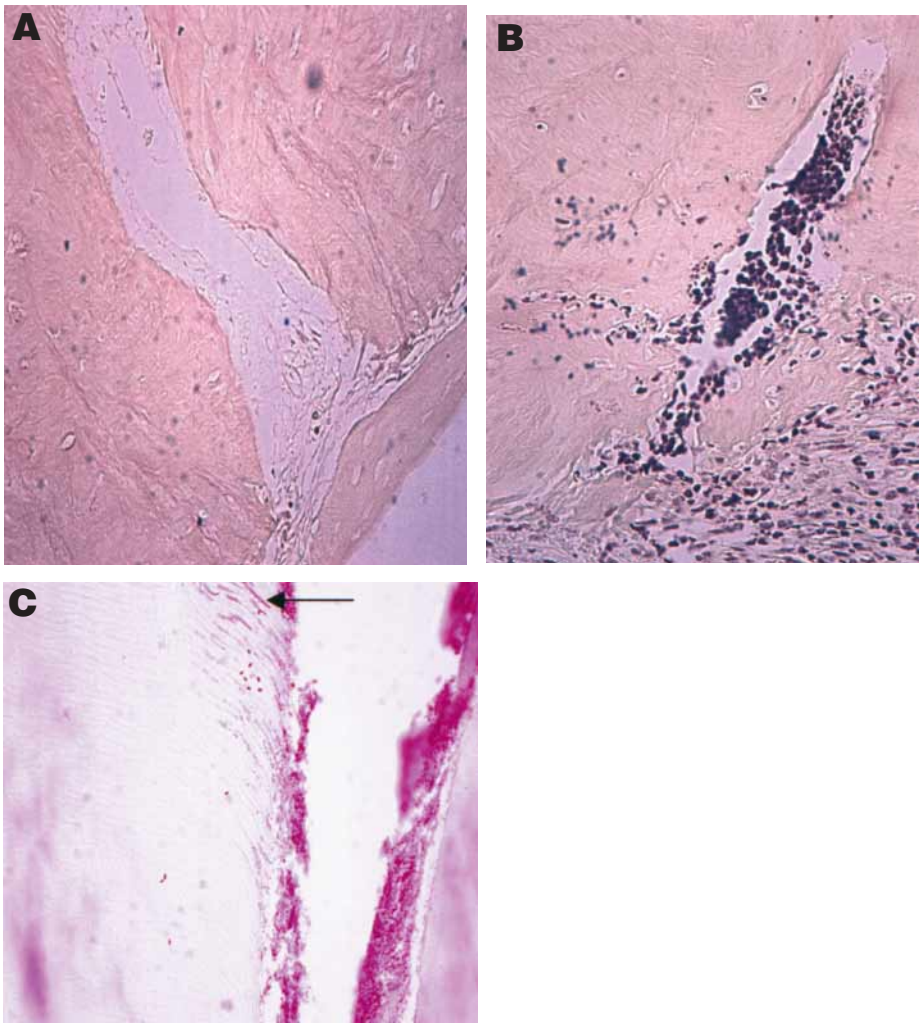

Fig 8. Photomicrograph of representative histologic sections stained with Brown and Brenn to detect bacteria. **A**, Apical area, nonexposed, noninfected tooth; **B**, apical area, exposed and infected tooth; **C**, illustrates the invasion of bacteria into the dentinal tubules in the apical one third of the root *(arrow)*.

The length of the distal roots in both groups was then determined from μ-CT images. Root length was significantly shorter (by 12.7%) in the experimental group compared with the controls ($P < .014$) (Table I). The amount of root resorption showed a weak but nonsignificant correlation with the extent of periradicular bony lesions (regression analysis) (Fig 6). This suggests that the 2 processes could be regulated differently within the periradicular milieu.

Histochemistry for clastic cells and bacteria

To demonstrate directly the presence of clastic cells associated with the resorptive process, sections were stained for TRAP activity. As shown in Fig 7, $TRAP^+$ multinucleated cells were observed on the root ends as well as on the osseous surfaces at the periphery of the periradicular lesions. The $TRAP^+$ cells on the root ends appeared to be somewhat smaller, with fewer nuclei, than the bone-associated osteoclasts.

The presence of bacteria in the dentinal tubules was evaluated by Brown and Brenn staining. Numerous Gram-negative bacteria were seen penetrating the dentinal tubules in the experimental group, compared with the controls (Fig 8). In some sections, bacterial invasion was seen toward the apical end of the dentinal tubules in which root destruction was taking place.

DISCUSSION

In the mouse model, the anatomic location of the incisive canal in the mandible does not allow periradicular lesions to expand significantly, except proximally and at the expense of the molar roots. Our findings clearly

showed that apical root resorption is a predictable finding in all teeth with pulpal infections. These findings were further substantiated by both two- and three-dimensional reconstructions of the roots by using μ-CT. TRAP+ clastic cells were associated with the processes of both bone and root resorption. Taken together, these findings show the loss of significant root structure in infected teeth and indicate that the mouse is a useful model for studying the mechanism of this process.

Apical inflammatory root resorption may include sites of activity on the root canal walls as well as the apical root surface and can have great clinical significance in endodontic practice. Clinically, the presence of apical root resorption is usually detected by radiographic means and may influence endodontic treatment decisions. The accuracy of radiographic diagnosis of resorption depends on several factors but can be verified conclusively only through examination of histologic sections of the affected teeth.[12] The histologic incidence of root resorption in clinical practice is always higher than when determined by radiography. In the study of Laux et al,[12] endodontists could detect radiographic signs of apical root resorption in fewer than 20% of teeth, whereas more than 80% of the teeth apices showed resorptive defects by histology. Several biologic and technical factors may contribute to the poor detection of apical root resorption with radiographs. These may include the size, location, and surrounding mineral content of the resorptive defects, anatomic variations of the jaw and teeth, and observer variation.[14-16] Small areas of resorption usually remain undetected compared with larger ones, and areas located on the proximal surfaces are more readily detected than those located on the buccal or lingual surfaces.

We identified the presence of TRAP+ clastic cells on the root surface as well as at the periphery of the lesion. TRAP+ cells on the distal root ends appeared to be smaller than the cells seen on the surrounding bone. Previous reports have also suggested that dentin- and cementum-resorbing cells (odontoclasts or cementoclasts) have fewer nuclei and smaller clear zones and are reduced in size compared with osteoclasts.[17] Although this has been attributed to the differences in composition of the dental tissues and bone, the reason for this finding is unknown.

Osteoclast formation and activation are regulated by local factors that are expressed at sites of inflammation. Osteoclast formation from precursor cells is principally up-regulated by macrophage colony-stimulating factor and the receptor-activator of NF-κB ligand (RANKL), both of which are expressed by osteoblasts/stromal cells after stimulation by resorptive signals such as IL-1, parathyroid hormone, and vitamin D3.[18] In murine periradicular lesions, inflammatory cells, particularly macrophages, express high levels of IL-1α, IL-1β, and tumor necrosis factor–α.[3,19] Inhibition of IL-1 activity by IL-1 receptor antagonist significantly reduces periradicular bone resorption.[20] Given the lack of a correlation between the extent of periradicular bone and root resorption (Fig 6), it is possible that these processes are to some extent regulated independently. It may be speculated that local tooth-associated factors (ie, bacteria within the dentinal tubules) may determine the extent to which root resorption occurs. In this regard, the continuous egress of microbial products through the tubules may provide the stimulus for the ongoing differentiation and activation of clastic cells in the periodontal ligament, resulting in further bone and root resorption.[1] Microbial products stimulate the expression of IL-1 and tumor necrosis factor–α, after interaction with *Toll*-like receptors on macrophages and other cell types.[21] This process may be further exacerbated by the resorption of cementum, which opens dentinal tubules, allowing them to communicate with cells of the periodontal ligament and alveolar bone.

An alternative pathway for osteoclast differentiation that has been proposed at inflammatory sites is the induction of RANKL in activated T cells.[22] T cells are present in periradicular lesions[8] and are activated by antigen processed by macrophages and other antigen-presenting cells. However, no differences in the amount of periradicular resorption were found in T-cell–deficient compared to T-cell–replete animals.[23,24] Resorption in this model therefore primarily reflects inflammatory cytokine expression by macrophages and other cell types, as a result of activation of innate immune pathways.

We thank Justine Dobeck for assistance with histology and Megan Mack for help in preparation of the manuscript.

REFERENCES

1. Nair P. Apical periodontitis: a dynamic encounter between root canal infection and host response. Periodontology 1997;13:121-48.
2. Stashenko P, Teles R, D'Souza R. Periapical inflammatory responses and their modulation. In: Alvares O, editor. Crit Rev Oral Biol Med; 1998. p. 498-521.
3. Kawashima N, Stashenko P. Expression of bone-resorptive and regulatory cytokines in murine periapical inflammation. Arch Oral Biol 1999;44:55-66.
4. Wang CY, Stashenko P. The role of interleukin-1 alpha in the pathogenesis of periapical bone destruction in a rat model system. Oral Microbiol Immunol 1993;8:50-6.
5. Hammarstrom L, Lindskog S. Factors regulating and modifying dental root resorption. Proc Finn Dent Soc 1992;88(suppl 1):115-23.
6. Domon T, Osanai M, Yasuda M, Seki E, Takahashi S, Yamamoto T, et al. Mononuclear odontoclast participation in tooth resorption: the distribution of nuclei in human odontoclasts. Anat Rec 1997;249:449-57.

7. Ne RF, Witherspoon DE, Gutmann JL. Tooth resorption. Quintessence Int 1999;30:9-25.
8. Yu SM, Stashenko P. Phenotypic characterization of inflammatory cells in induced rat periapical lesions. J Endod 1987;13:535-40.
9. Wang CY, Stashenko P. Kinetics of bone-resorbing activity in developing periapical lesions. J Dent Res 1991;70:1362-6.
10. Sasaki H, Hou L, Belani A, Wang CY, Uchiyama T, Mueller R, et al. IL-10 but not IL-4 suppresses infection-stimulated bone resorption in vivo. J Immunol 2000;165:3626-30.
11. Balto K, Sasaki H, Stashenko P. Interleukin-6 deficiency increases inflammatory bone destruction. Infect Immun 2001;69:744-50.
12. Laux M, Abbott PV, Pajarola G, Nair P. Apical inflammatory root resorption: a correlative radiographic and histological assessment. Int Dent J 2000;33:483-93.
13. Balto K, Muller R, Carrington DC, Dobeck J, Stashenko P. Quantification of periapical bone destruction in mice by micro-computed tomography. J Dent Res 2000;79:35-40.
14. Bender I. Factors influencing the radiographic appearance of bony lesions. J Endod 1982;8:161-70.
15. Reit C, Hollender L. Radiographic evaluation of endodontic therapy and the influence of observer variation. Scand J Dent Res 1983;91:205-12.
16. Tidmarsh BG. Radiographic interpretation of endodontic lesions: a shadow of reality. Int Dent J 1987;37:10-5.
17. Anan HAA, Maeda K. An enzyme histochemical study of the behavior of rat bone cells during experimental apical periodontitis. J Endod 1993;19:83-6.
18. Takahashi N, Udagawa N, Suda T. A new member of tumor necrosis factor ligand family, ODF/OPGL/TRANCE/RANKL, regulates osteoclast differentiation and function. Biochem Biophys Res Commun 1999;256:449-55.
19. Akamine A, Hahiguchi I, Toriya Y, Maeda K. Immuno-histochemical examination on the localization of macrophages and plasma cells in induced rat periapical lesions. Endod Dent Traumatology 1994;10:121-8.
20. Stashenko P, Wang CY, Tani-Ishii N, Yu SM. Pathogenesis of induced rat periapical lesions. Oral Surg Oral Med Oral Pathol 1994;78:494-502.
21. Kopp EB, Medzhitov R. The Toll-receptor family and control of innate immunity. Curr Opin Immunol 1999;11:13-8.
22. Horwood HJ, Kartsogiannis V, Quinn JM, Romas E, Martin TJ, Gillespie MT. Activated T lymphocytes support osteoclast formation in vitro. Biochem Biophys Res Commun 1999;265:144-50.
23. Wallstrom JB, Torabinejad M, Kettering J, McMillan P. Role of T cells in the pathogenesis of periapical lesions: a preliminary report. Oral Surg Oral Med Oral Pathol 1993;76:213-8.
24. Hou L, Sasaki H, Stashenko P. B-cell deficiency predisposes mice to disseminating anaerobic infections: protection by passive antibody transfer. Infect Immun 2000;68:5645-51.

Reprint requests:

P. Stashenko, DMD, PhD
The Forsyth Institute
140 The Fenway
Boston, MA 02115
pstashenko@forsyth.org